



*Supplement of*

**A predictive thermodynamic framework of cloud droplet activation for chemically unresolved aerosol mixtures, including surface tension, non-ideality, and bulk–surface partitioning**

Nønne L. Prisle

*Correspondence to:* N. L. Prisle ([nonne.prisle@oulu.fi](mailto:nonne.prisle@oulu.fi))

The copyright of individual parts of the supplement might differ from the article licence.

## **S1 Insoluble surfactant model with constant surface tension**

Ruehl et al. (2016) described surfactant behavior in growing droplets with an insoluble film model. Experimental data of corresponding subsaturated humidity and growing droplet size necessary to fit their model parameters are not available for mixtures of Nordic Aquatic Fulvic Acid (NAFA) and NaCl. To make a tentative comparison to the surface-based framework of Ruehl et al. (2016), the simple partitioning model (S) is here implemented with a constant reduced surface tension corresponding to 95% and 80% of the pure water value, similarly to the approach of Davies et al. (2019). Predicted critical supersaturations for NAFA–NaCl particles of different sizes and compositions are shown in panels (c) and (d) of Fig. S1 and compared to the same experimental values of Kristensen et al. (2014) also shown in Fig. 1. It is clear that increasingly reduced droplet surface tension better reproduces experimental CCN activation of pure NAFA particles, compared to the assumption of pure water surface tension. However, across all NAFA–NaCl particle mixtures, a constant reduced surface tension lead to overestimation of CCN activity. Even lower surface tensions were also applied, but produced still poorer agreement with experiments and these model results are therefore not shown here. This highlights how the insoluble surfactant model with a constant reduced surface tension fails to capture the changing NAFA–NaCl aqueous droplet states as they grow and dilute.

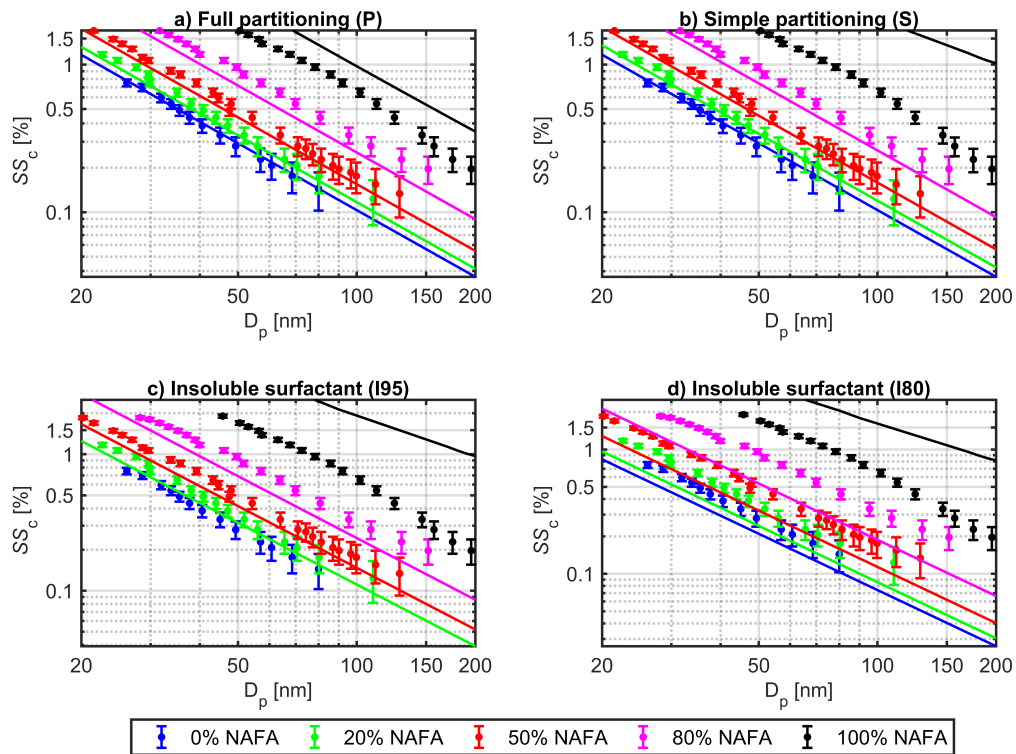


Figure S1: Sensitivity of Köhler model calculations with the simple partitioning model to the assumed constant value of the droplet surface tension. For reference is shown (a) the full partitioning model (P) and (b) the simple partitioning model (S) representing an insoluble surfactant and droplet surface tension equal to that of pure water. Calculations are shown for an insoluble surfactant (I) with droplet surface tension reduced by (c) 95% and (d) 80%, compared to pure water. In each case, model results are compared to experimental values from Kristensen et al. (2014).

## S2 Bulk composition of droplets at the point of activation

Figure S2 presents mass concentrations of (a) NAFA and (b) NaCl in the droplet bulk,  $C_{\text{NAFA}}$  and  $C_{\text{NaCl}}$  (both in  $\text{g L}^{-1}$ ), calculated at the critical point of activation  $d_c$  for the same particles with dry diameters of 50 nm and compositions  $W_{\text{p,NAFA}}$  as shown in Fig. 2. These are the solute concentrations governing the evaluated droplet surface tensions and water activities at activation. For the non-partitioning salt,  $C_{\text{NaCl}}$  is determined by the total amount of NaCl in the dry particle, given from  $W_{\text{p,NAFA}}$ , and the droplet dilution state at activation,  $GF_c$  (Fig. 2c). For models (P), (S) and (I),  $C_{\text{NAFA}}$  is in addition affected by bulk depletion from the size-dependent or step-wise bulk/surface partitioning of NAFA. In calculations with models (S) and (I), the bulk NAFA concentration is vanishing due to complete partitioning to the droplet surface, however, also for the comprehensive partitioning model (P) are NAFA bulk concentrations nearly vanishing at the point of activation across all dry particle compositions. Qualitatively similar results were obtained for other dry particle sizes. For larger particles, concentrations at droplet activation are even more dilute than those presented here for 50 nm particles.

In model (K), concentrations of *both* NAFA and NaCl in activating droplets increase with  $W_{\text{p,NAFA}}$ , except for particles with the very largest dry NAFA fractions. This reflects how particles activate for still more concentrated droplet compositions, as seen in Fig. 2 (c). Across the all models, evaluated  $C_{\text{NaCl}}$  at droplet activation for a given dry particle composition follow the trend in  $GF_c$ . In particular, for all models except (B), activating droplets become more concentrated in the inorganic salt, even if  $W_{\text{p,NaCl}}$  decreases. For calculations with (B),  $C_{\text{NAFA}}$  increases with  $W_{\text{p,NAFA}}$  and decreasing  $GF_c$ , as expected.  $C_{\text{NaCl}}$  first decreases slightly, as the amount of NaCl in the particles decreases with increasing  $W_{\text{p,NAFA}}$ , reflecting also a state of increasing, or relatively high, dilution, as activation occurs for large  $d_c$  when droplet surface tension is increasingly reduced (Fig. 2d). A discontinuous increase is seen with (B) for both  $C_{\text{NAFA}}$  and  $C_{\text{NaCl}}$  at  $W_{\text{p,NAFA}} = 0.85$ , reflecting the sudden decrease in  $GF_c$  seen in Fig. 2 (c) as droplet activation shifts from the local Köhler curve maximum at the larger  $d_c$  to that at the smaller (Figs. 3 and 4). For all models,  $C_{\text{NaCl}}$  show an inflection point for the largest  $W_{\text{p,NAFA}}$ , where concentrations eventually fall, as decreasing dilution can no longer counter the decreasing total NaCl content in the droplets. This inflection point is visible in the Raoult terms of the partitioning models (P), (S), and (I) seen in Fig. 2 (b), but not strong enough to translate into a similar inflection the Raoult terms of the bulk solution models (B) and (K).

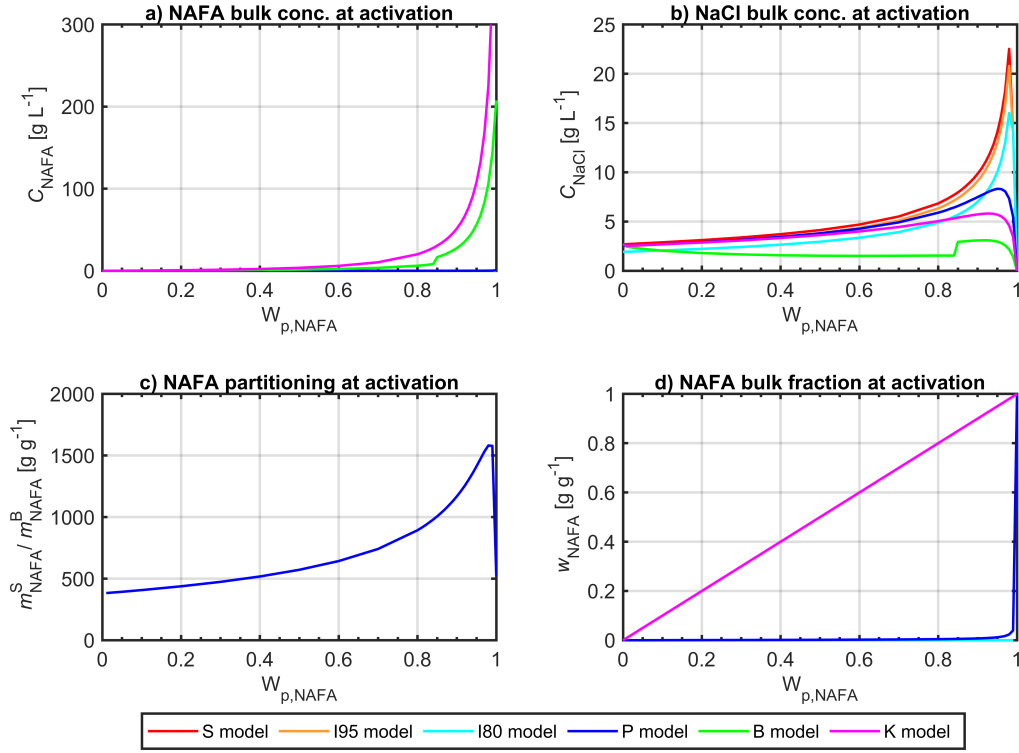


Figure S2: Mass concentrations  $C_i$  (in  $g L^{-1}$ ) of (a) NAFA and (b) NaCl in activating droplets, calculated with the different models (P), (S), (I), (B), and (K), described in Section 2.4, for dry particles with diameters of 50 nm. For the same particles are also shown (c) NAFA surface partitioning factor  $m_{NAFA}^S / m_{NAFA}^B$ , and (d) mass fraction of bulk solute comprised by NAFA,  $w_{NAFA} = m_{NAFA}^S / (m_{NAFA}^S + m_{NaCl}^S)$ , evaluated at the point of droplet activation.

### S3 Droplet properties along the Köhler curves

Figures S3 and S4 show the NAFA surface partitioning factor  $m_{\text{NAFA}}^S/m_{\text{NAFA}}^B$  and water activity  $a_w$ , respectively, calculated with each surfactant representation along the Köhler curves shown in Fig. 3 for 50 nm dry particles with compositions  $W_{\text{p,NAFA}} =$  (a) 0.20, (b) 0.50, (c) 0.80, and (d) 0.95. Results are discussed in Section 3.3. In general, the submicron growing droplets are strongly depleted from bulk/surface partitioning of NAFA, which is reflected in water activities approaching 1 at still earlier stages of droplet growth as the NAFA fraction in the dry particles increases.

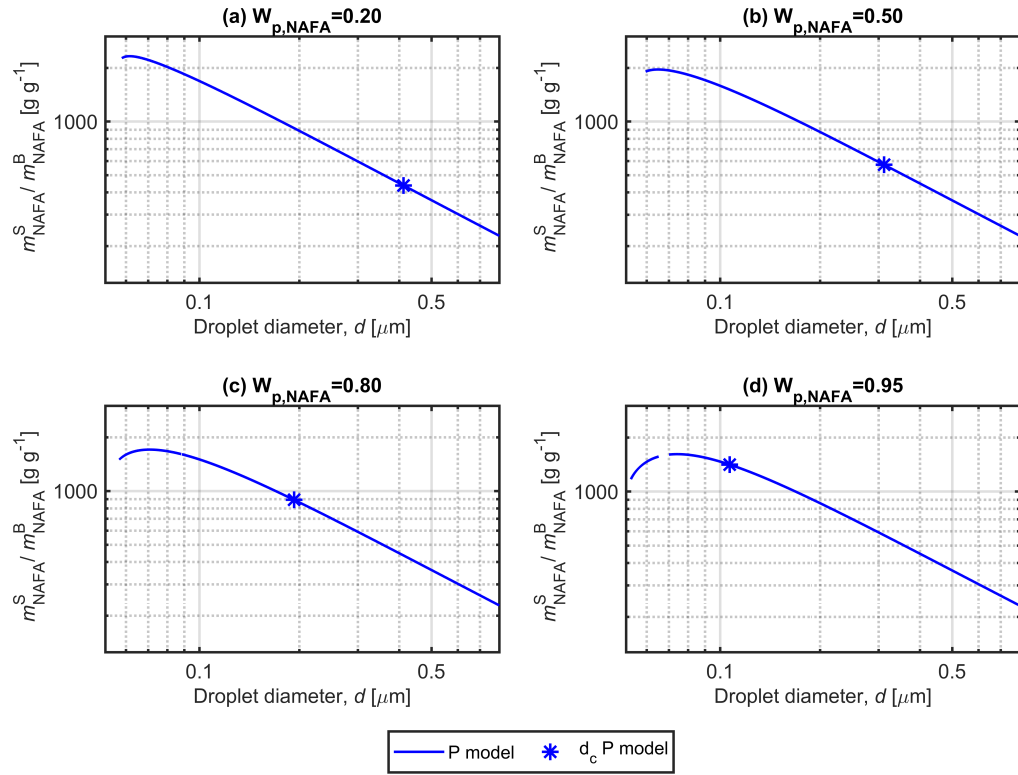


Figure S3: NAFA surface partitioning factor  $m_{\text{NAFA}}^S / m_{\text{NAFA}}^B$  along Köhler curves for growing aqueous NAFA–NaCl droplets formed from 50 nm dry particles with different NAFA mass fractions, (a) 0.20, (b) 0.50, (c) 0.80, and (d) 0.95, calculated with the full mass-based partitioning model (P). The calculated critical points of droplet activation ( $SS_c$ ) presented in Figs. 1, 3 and S1 are indicated with asterisks on the curves for each droplet.

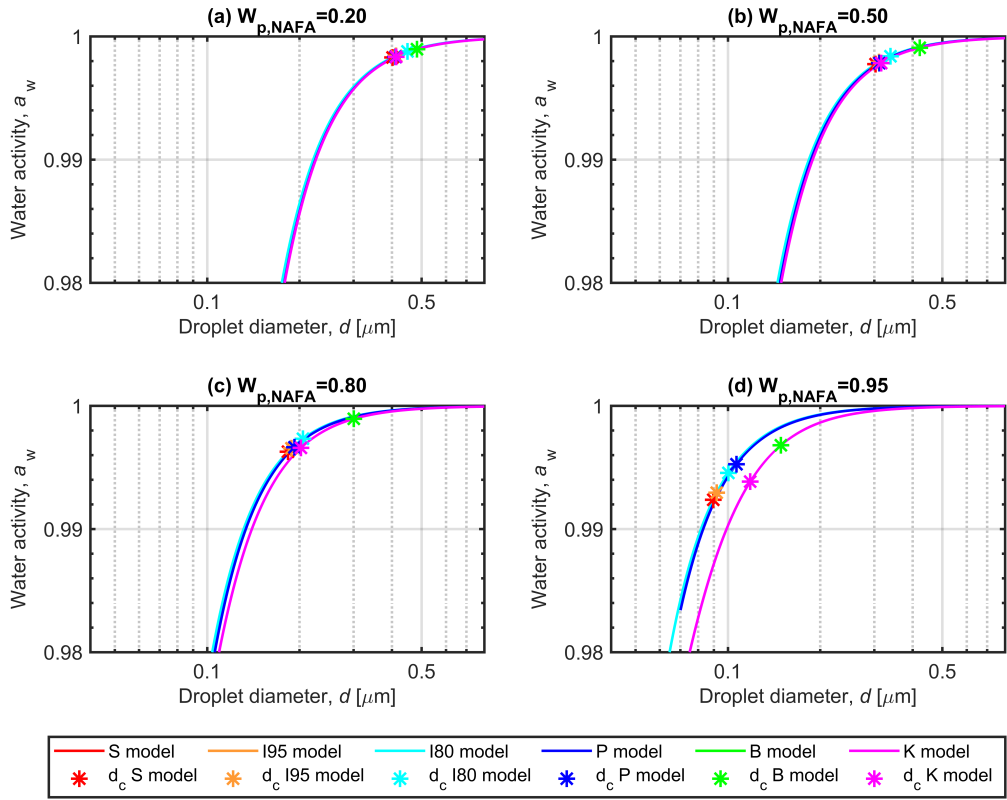


Figure S4: Water activity along the Köhler curves for growing aqueous NAFA–NaCl droplets formed from 50 nm dry particles with NAFA mass fractions of (a) 0.20, (b) 0.50, (c) 0.80, and (d) 0.95, calculated with the different models described in Section 2.4. The calculated critical points of droplet activation ( $SS_c$ ) presented in Figs. 1, 3 and S1 are indicated with asterisks on the curves for each droplet.

## S4 Surface tension of NAFA solutions

NAFA is a surface active commercially available reference mixture and significantly reduces surface tension in macroscopic aqueous solutions, as is also the case for other model HUmic LIke Substances (HULIS) like Suwannee River Fulvic Acid (SRFA) and Humic acids (e.g. Kiss et al., 2005; Aumann et al., 1967; Kristensen et al., 2014). Figure S5 (a) shows the variation in aqueous surface tension as a function of NAFA mass concentration in solution modeled using the continuous ternary Eq. 8 (Section 2.3.1) and compared to the underlying measurements of Kristensen et al. (2014) for macroscopic bulk solutions with mass mixing ratios of 20, 50, 80, and 100% NAFA relative to NaCl. To obtain a smooth fit with continuous independent variations in both NAFA and NaCl concentrations, the ternary parametrization does not always represent data quite as well as the individual fits of Kristensen et al. (2014) to one dimensional concentration domains with fixed  $w_{\text{NAFA}}$  (not shown), especially for dilute solutions. To facilitate comparison with the experimental data, surface tensions in Fig. S5 are predicted for 298 K, whereas calculations of CCN activity in this work are made for temperatures of 303 K, yielding potentially lower aqueous surface tensions due to the temperature dependence of Eq. 8. The effect on Köhler calculations is however negligible (see Section S6 for more details on model sensitivity).

Surface tension of NAFA–NaCl solutions is well described with the Szyszkowski-type equation (Eq. 8) as expected for a surface active solute with non-vanishing aqueous solubility. At a given  $C_{\text{NAFA}}$ , the surface tension reduction increases with concentration of NaCl (i.e. with decreasing  $w_{\text{NAFA}}$ ) until at least 80% of the solute mass is comprised by NaCl. This is a clear demonstration of *salting out* (see e.g. Tuckermann, 2007) of NAFA by the inorganic salt in these solute composition and concentration ranges. Salting out is likely caused by increased non-ideality (ionic strength) in solutions with larger NaCl concentrations affecting the solubility and/or surface propensity of NAFA by enhancing the activity ( $a_{\text{NAFA}} = \gamma_{\text{NAFA}}x_{\text{NAFA}}$ , where  $\gamma_{\text{NAFA}} > 1$ ) in solution.

Figure S5 (b) shows the variation in ternary surface tension fitting parameters given by Eqs. 9 and 10 across the full range of NAFA solute mass fractions  $w_{\text{NAFA}}$ . By analogy to the Szyszkowski equation (Szyszkowski, 1908), parameter  $q_{\text{st1}}$  can be interpreted as related to the maximum surface excess  $\Gamma_{\text{NAFA}}^{\text{max}}$  (notably, defined on a mmol/m<sup>2</sup> concentration scale) by

$$q_{\text{st1}} = RT\Gamma_{\text{NAFA}}^{\text{max}}, \quad (1)$$

and parameter  $q_{\text{st2}}$  as the (inverse of the) surface activity coefficient (with respect to a mass-concentration scale and infinite dilution reference state), see also Aumann et al. (1967). Fig. S5 (b) shows how NAFA surface activity is predicted

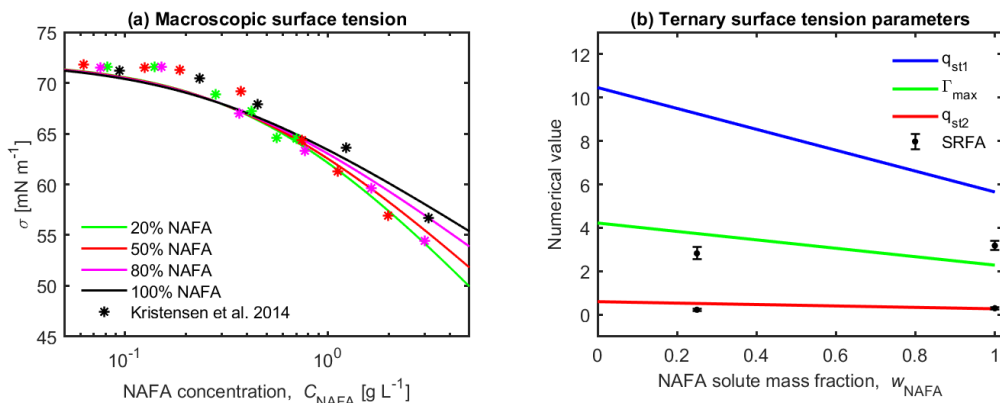


Figure S5: Macroscopic surface tension of aqueous NAFA–NaCl solutions: (a) Surface tension as function of NAFA mass concentration in solutions with different NAFA and NaCl mixing ratios, as predicted with the ternary parametrization in Eqs. 8–10 for 298 K, and compared to data from Kristensen et al. (2014). (b) Variation in the Szyszkowski fitting parameters given in Eqs. 9 and 10 and the related maximum surface excess  $\Gamma_{\text{NAFA}}^{\text{max}}$  from Eq. S1 with NAFA mass fraction  $w_{\text{NAFA}}$  relative to NaCl in solution. Similar data for Suwannee River Fulvic Acid from Aumann et al. (1967) is shown for comparison.

to increase (the inverse of  $q_{\text{st2}}$  increases) with increasing  $w_{\text{NAFA}}$ , while the corresponding maximum surface excess (and  $q_{\text{st1}}$ ) simultaneously decreases. The latter effect may be caused by concurrent increased depletion of salt ions from the aqueous surface as the salt fraction increases. Interestingly, very similar values are found here for both  $\Gamma^{\text{max}}$  and surface adsorption parameter  $q_{\text{st2}}$  as for Suwannee River Fulvic Acid in both binary aqueous solution and a 25% solute mass mixture with NaCl by Aumann et al. (1967). Their data for SRFA has been included in Fig. S5 (b) for comparison.

It was seen already in Fig. S2 how activating droplets formed on NAFA containing particles are predicted to be fairly dilute aqueous solutions, with bulk solute compositions  $\{w_i\}$  significantly different from the original dry particle composition  $\{W_{p,i}\}$  when NAFA bulk–surface partitioning is taken into account. For example, mass concentrations of NAFA and NaCl are 0.0066 gL<sup>-1</sup> and 3.80 gL<sup>-1</sup>, respectively, at the point of droplet activation, calculated with model (P) for 50 nm particles with dry mass fractions of 50% NAFA. For 100 and 150 nm particles of the same composition, the corresponding values (not shown) are 0.0065 and 0.0064 gL<sup>-1</sup> NAFA, and 1.34 and 0.736 gL<sup>-1</sup> NaCl. The relative solute mass fractions of NAFA  $w_{\text{NAFA}}$  in the activating droplets are thus 0.0017, 0.0049, and

0.0086 for the 50, 100, and 150 nm dry particles, respectively.

Modeled surface tensions for aqueous solutions with NAFA solute mass fractions  $w_{\text{NAFA}}$  of 0.001, 0.01, 0.1, and 1, respectively, are shown in Fig. S6 as functions of surfactant mass concentration. There are virtually no differences between the variation of surface tensions with  $C_{\text{NAFA}}$  modeled for different mixing ratios  $w_{\text{NAFA}} < 0.1$  (all fall under the pink line for  $w_{\text{NAFA}} = 0.1$ ). Solute mixing states  $w_{\text{NAFA}} > 0.1$  are not realized for activating droplets when partitioning is included and these results are shown in Fig. S6 merely to illustrate the surfactant fractions at which changes due to solute mixing state do begin to occur.

In the NAFA concentration range up to  $10^{-2} \text{ g L}^{-1}$ , predicted ternary surface tensions are virtually identical to  $\sigma_w$ . These are solutions representative of droplet bulk concentrations at  $d_c$  for particles with a dry NAFA mass fraction of 50%. For some of the highest fractions of NAFA, as in the case of  $W_{\text{p,NAFA}} = 0.95$ , the concentrations predicted with model (P) in activating droplets formed on 50, 100, and 150 nm dry particles are 0.1121, 0.1271, and 0.1306  $\text{g L}^{-1}$  of NAFA, and 9.2485, 3.6409, and 2.0446  $\text{g L}^{-1}$  of NaCl, respectively, and the corresponding values of  $w_{\text{NAFA}}$  are 0.0120, 0.0337, and 0.0600.

The surface tension values for solution compositions representative of activating NAFA–NaCl droplets shown in Fig. S6 are not constrained by the measurement data of Kristensen et al. (2014) and Lin et al. (2020). In model (P),  $w_{\text{NAFA}}$  is significantly decreased from  $W_{\text{p,NAFA}}$  of the original dry particle, due to bulk depletion of NAFA, but not of the salt, and typically  $C_{\text{NAFA}} \ll C_{\text{NaCl}}$ . An important implication of this is that the ternary surface tension and water activity parametrizations used for calculating properties during droplet growth and activation are both extrapolated far beyond the well-constrained composition domains for making the comprehensive partitioning calculations in this work. As a consequence, it is strongly recommended that this potentially large change in droplet composition from corresponding macroscopic solutions is taken into consideration when measuring aqueous surface tension of various organic aerosol components for the purpose of analyzing or predicting aerosol CCN activity. There are also, however, significant challenges involved in measuring accurate surface tension–concentration isotherms for such low organic concentrations and in preparing samples with the appropriate well-defined organic–inorganic mixing ratios.

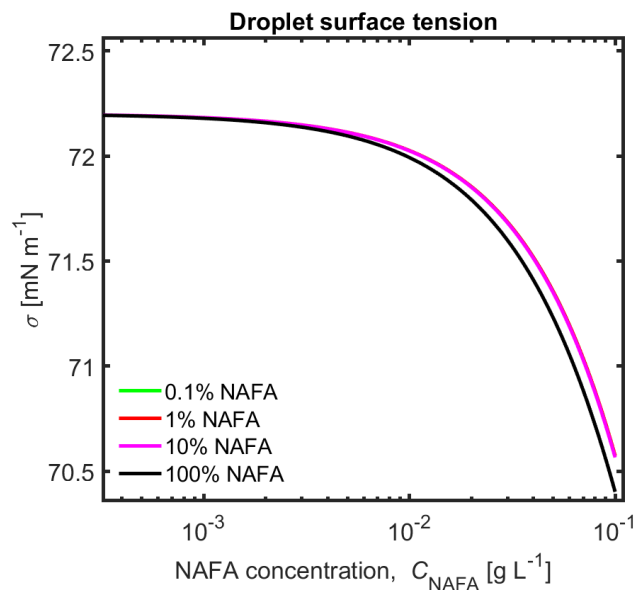


Figure S6: Surface tensions as function of NAFA mass concentration  $C_{\text{NAFA}}$  predicted with Eqs. 8–10 for aqueous solutions with NAFA solute mass fractions  $w_{\text{NAFA}}$  of 0.001, 0.01, 0.1, and 1, relative to NaCl, corresponding to bulk compositions predicted for activating droplets when bulk/surface partitioning is considered using the full mass-based model (P).

## S5 Dynamic surface tension effects

Kristensen et al. (2014) and Lin et al. (2020) report that aqueous NAFA surface tensions measured with the pendant drop tensiometer decrease with time after formation of the sample surface. This is likely due to both dynamic effects of surface adsorption from diffusion and structural rearrangements in the surface phase, as well as potentially to increasing concentrations of the pendant drop samples from evaporation of water over the course of measurements. In this work, model predictions are compared with measurements of CCN activity for mixed NAFA–NaCl particles reported by Kristensen et al. (2014). Surface equilibration in the microscopic activating cloud droplets is considered to be diffusion controlled (Alvarez et al., 2012) and much faster than for the macroscopic (millimeter-sized) droplets measured with the pendant drop tensiometer (Alvarez et al., 2010). However, potential dynamic effects related to diffusion of especially the high average molar mass NAFA component to the droplet surface, could be speculated to lead to incomplete (non-equilibrium) partitioning of NAFA during droplet activation in the CCN counter.

Fitting parameters for the surface tension parametrization (Eqs. 8–10) used in the present calculations were obtained from measurement data corresponding to times  $t = 600$  s after generation of the pendant drops. Droplet activation takes place during exposure times of about 1 s in the CCN counter, depending on the particle size and required critical supersaturation (Kristensen et al., 2014). Following the considerations of Prisle et al. (2008), the ratio of the measurement time scales between the pendant drop surface tension measurements corresponding to 600 s and the cloud droplet activation measurements is estimated to be of the same order of magnitude as the ratio of diffusion distances in the samples, as given by the diameter ratio of the droplet systems involved in the two types of measurement, i.e. (pendant drop size/activating droplet size)  $\sim$  (pendant drop measurement time/droplet activation measurement time)  $\sim 10^2$ – $10^3$ . With this simple argument, any potential dynamic effects related to diffusion of NAFA to the droplet surface are therefore assumed to be at least comparable between the surface tension parametrizations used for the model calculations and the droplet activation measurements, if present at all.

At the selected measurement time lapse of  $t = 600$  s, generally the steepest and the majority of the total dynamic surface tension decrease had occurred in the NAFA–NaCl solutions, indicating that dynamic effects of surface adsorption due to diffusion are limited beyond this point. Because surface tension measurement data corresponding to measurement times of 600 s were available from Kristensen et al. (2014) and Lin et al. (2020) for the widest range of solution compositions, these data were used rather than those corresponding to even longer measurement times.

The applicability of partitioning models for CCN measurements has occasionally been questioned, due to the long equilibration times of surface tension in some (macroscopic) systems (Noziere et al., 2014; Fainerman et al., 2002; Wen et al., 1998; Coltharp and Franses, 1996; Van den Bogaert and Joos, 1980, 1979), compared to particle and droplet residence times in commonly used cloud condensation nucleus counters (Prisle et al., 2008; Kristensen et al., 2014). Recently, Lin et al. (2020) presented a detailed analysis of the effects of using surface tension parametrizations corresponding to different equilibration time scales in Köhler calculations. They observe complex relations between the influence of changing droplet size and composition, surface adsorption, and time-evolving surface tension. A clear progression of predicted surface adsorption in droplets is seen, as expected, when using surface tension parametrizations corresponding to successively longer equilibration times, but the effects of this surface adsorption on the individual Kelvin and Raoult terms of the droplet growth curve nearly cancel at every time step. In the atmosphere, the time a particle spends in an updraft below cloud up to cloud base is also on the order of only

a few seconds, similar to the residence time in the CCN counter. It is therefore conceivable, that dynamic effects could have similar impact in the atmosphere as predicted by Lin et al. (2020). Currently, there is no standard experiment that would allow independent verification of these predictions. Furthermore, no other comprehensive set of surface tension measurements exists to enable similar calculations as for the NAFA–NaCl mixtures, with considerations of time-evolution of bulk/surface partitioning in connection with CCN activation. Therefore, the general nature of such dynamic phenomena is currently unclear.

## S6 Model sensitivities

The sensitivity of Köhler model calculations – in particular those using the comprehensive mass-based partitioning model (P) – was tested to variation in key input parameters, including surface tension equation, assumed NAFA mass density and average molar mass, droplet temperature, and impurities in assumed dry particle composition. Selected results are discussed below.

### S6.1 Assumed density of NAFA

Tracing back to experimental (mobility) diameter based particle sizing, the masses ( $m_i$ ) of dry particle constituents ( $i$ ) initialize the calculations of droplet growth. Given by Eq. 3 (Section 2.1), the assumed NAFA mass density  $\rho_{\text{NAFA}}$  affects Köhler model calculations *via* the predicted amounts of both NAFA and NaCl solutes present in (spherical) particles of a given dry size  $D_p$  and corresponding volume. For a given particle composition in terms of relative NAFA and NaCl mass fractions  $W_{\text{p,NAFA}} + W_{\text{p,NaCl}} = 1$ , the volume fractions of each dry particle component  $i = \text{NAFA, NaCl}$  are

$$\epsilon_i = \frac{W_{\text{p},i}}{\rho_i} \left( \frac{W_{\text{p,NAFA}}}{\rho_{\text{NAFA}}} + \frac{W_{\text{p,NaCl}}}{\rho_{\text{NaCl}}} \right)^{-1}. \quad (2)$$

A higher mass density of NAFA therefore increases the *volume* fractions  $\epsilon_i$  of both NAFA and NaCl in particles of a given dry volume and fixed relative *mass* fractions  $W_{\text{p},i}$ , according to Eq. S2. Consequently, higher values of  $\rho_{\text{NAFA}}$  affect the amounts of both soluble salt  $m_{\text{NaCl}}^T$  and surface active NAFA solute  $m_{\text{NAFA}}^T$  assumed to be present in the particles from the onset of droplet growth.

Figure S7 (a) shows calculated critical supersaturations with model (P), assuming a density for NAFA of  $1.6 \text{ g cm}^{-3}$  (base case), corresponding to a density similar to that of Suwannee River Fulvic Acid (SRFA), another common reference humic substance (Dinar et al., 2006), and  $1.2 \text{ g cm}^{-3}$ , a value similar to that assumed for the  $\text{C}_8 - \text{C}_{12}$  FAS (e.g. Prisle et al., 2010, and references herein),

which are significantly smaller surfactant entities than NAFA. Due to the much higher average molar mass estimated for NAFA (Mäkelä and Manninen, 2008) than for the FAS, the value of  $1.2 \text{ g cm}^{-3}$  is believed to be a lower (and likely too low) reasonable limit for  $\rho_{\text{NAFA}}$ . The NAFA density assumption does have a small effect on calculated  $SS_c$ , with the lower density leading to higher critical supersaturations, as expected. Due to the low overall influence of NAFA on droplet activation properties, the effect is likely caused mainly by the smaller amounts of soluble NaCl assumed to be present in dry particles of a given size and composition, when assuming the lower density value for NAFA, according to Eq. S2.

## S6.2 Assumed average molar mass of NAFA

Formulating the Gibbs adsorption equation on a mass basis introduces the molecular masses  $M_i$  of each droplet constituent  $i$ . Therefore, an assumption of the average molar mass is needed for the unresolved components, here NAFA, as  $\bar{M}_{\text{NAFA}}$ . The average molar mass of NAFA was estimated by Mäkelä and Manninen (2008) as  $4266 \text{ g mol}^{-1}$  across a distribution of masses identified in the mixture, whereas those of SRFA (Dinar et al., 2006) and of atmospheric HULIS (Kiss et al., 2003) have been estimated to be considerably lower. The sensitivity of calculations with model (P) was tested to decreasing the assumed NAFA average molar mass to  $2000 - 1000 \text{ g mol}^{-1}$  and, as a representative value for the average molar mass of SRFA and atmospheric HULIS, and as an absolutely lowest bound to  $500 \text{ g mol}^{-1}$ .

Results of sensitivity in calculated  $SS_c$  as a function of 50 nm dry particle composition are shown in Fig. S7 (b). The difference between 500 and  $4266 \text{ g mol}^{-1}$  represents a dramatic order-of-magnitude change in assumed average properties of the NAFA mixture and for particles with NAFA mass fractions above about 80%, it does influence calculated activation properties. Due to the very high average molar mass of NAFA, combined with the mixture's significant impact on surface tension, the partitioning of a single NAFA mass unit ("average molecule") in a few cases affects the outcome of calculations. This specifically happens for the smallest particles with the highest NAFA fractions  $W_{\text{NAFA}}$ , which activate as very small and highly bulk-depleted droplets. The effect is much less pronounced for larger particles, but for consistency with other results presented, and to highlight the largest differences possible, model results are here shown for the most sensitive small particle sizes. Experimental values of  $SS_c$  from Kristensen et al. (2014) for particles with approximate dry sizes of 50 nm are shown for reference. A potential difference in NAFA molar mass between the samples measured by Mäkelä and Manninen (2008) and Kristensen et al. (2014), or a

similar variation within a given NAFA sample used in experiments, in principle could reconcile calculations using (P) with experimental  $SS_c$  via a similar mechanism. However, as the reported uncertainty on measured NAFA  $SS_c$  in terms of experimental standard deviations is low, the influence on sample variability on experimental CCN activity therefore cannot be very large.

### S6.3 Droplet temperature

The temperature  $T$  (in Kelvin) inside the cloud condensation nucleus counter (CCNC), where particle activation is taking place and measured, depends on the supersaturation ( $SS = (S - 1) \cdot 100\%$ ) inside the instrument, approximately according to the linear relationship (T.B. Kristensen, personal communication)

$$T = 7.4 SS + 298.75 . \quad (3)$$

Over the range of particle sizes measured by Kristensen et al. (2014), the activation temperature therefore varies roughly between 298 K for the lowest supersaturations and 313 K for the highest.

In the Köhler calculations, a constant temperature of 303.15 K was used for all particle sizes to evaluate their critical supersaturations from the equilibrium Köhler curve. Temperature affects calculations both indirectly through the surface tension, which in this range increases with decreasing temperature according to temperature-dependent surface tension of pure water (in  $\text{mN m}^{-1}$ )  $\sigma_w = 93.6635 + 0.009133 T - 0.000275 T^2$  (Dillmann and Meier, 1991; Vanhanen et al., 2008) and directly through the Kelvin term of the Köhler equation (Eq. 1 in Section 2.1), which also decreases for increasing temperature. Sensitivity of model (P) was tested to variations in temperature between 298 and 313 K. Results are shown in Fig. S7 (c) for calculated critical supersaturations as function of 50 nm dry particle NAFA mass fraction. For lower temperatures, the calculated  $SS_c$  are slightly higher, and *vice versa*, as expected, but overall the temperature variation in this range has only minor influence on results.

### S6.4 Surface tension parametrization

Models (P) and (B) include concentration dependent droplet surface tension and the sensitivity was tested of calculations to the functional form of the ternary surface tension fit, as well as of the fitting parameters  $q_{st1}$  and  $q_{st2}$ . Eq. 8 implicitly accounts for the effect of NaCl on surface tension via the dependence of fitting parameters on solute mixing ratio  $w_{\text{NAFA}}$ , as given by Eqs. 9 and 10. A ternary

parametrization was also used with an explicit account for NaCl with an additional binary salt term as

$$\sigma = \sigma_w + \left( \frac{d\sigma_{\text{NaCl}}}{dc_{\text{NaCl}}} \right) c_{\text{NaCl}} - q_{\text{st1}} \ln(1 + C_{\text{NAFA}}/q_{\text{st2}}), \quad (4)$$

with fitting parameters

$$q_{\text{st1}} = 9.995 - 4.259w_{\text{NAFA}} - 0.03879w_{\text{NAFA}}^2 \quad (5)$$

and

$$q_{\text{st2}} = 0.5919 - 0.432w_{\text{NAFA}} + 0.1175w_{\text{NAFA}}^2. \quad (6)$$

Here,  $c_{\text{NaCl}}$  is the salt molal concentration in  $[\text{mol} (\text{kg water})^{-1}]$ ,  $C_{\text{NAFA}}$  is the NAFA mass concentration in  $[\text{g L}^{-1}]$ , and the binary NaCl surface tension gradient  $\frac{d\sigma_{\text{NaCl}}}{dc_{\text{NaCl}}} = 1.61 \text{ mN m}^{-1}/\text{mol} (\text{kg water})^{-1}$  is calculated from data from Low (1969) as was done by Prisle et al. (2010).

Results are shown in Fig. S7 (d) for calculated critical supersaturations as function of 50 nm dry particle NAFA mass fraction. Calculations are somewhat sensitive to the functional form of the surface tension parametrization and fitting parameters. The maximum sensitivity is comparable to the experimental uncertainty reported by Kristensen et al. (2014) and, as expected, seen for particle compositions with large fractions of NAFA, but only in mixtures with NaCl, where interactions between the solutes are expected to be most prominent. Eq. S4 was therefore also tested with a different set of quadratic parameters,  $q_{\text{st1}} = 72.13 - 158.4w_{\text{NAFA}} + 93.52w_{\text{NAFA}}^2$  and  $q_{\text{st2}} = 6.556 - 15.51w_{\text{NAFA}} + 9.431w_{\text{NAFA}}^2$ . Results are qualitatively similar to those for the parameter values given by Eqs. S5 and S6 and only shown for this case in Fig. S7 (d).

Model sensitivity is greater for (P), where critical droplets are predicted to be more concentrated and with bulk solute compositions  $\{w_i\}$  which are dramatically changed from the nominal dry particle compositions  $\{W_{p,i}\}$ . For these droplets, the explicit salt term leads to surface tensions slightly above that of pure water, as  $C_{\text{NAFA}} \rightarrow 0$  due to bulk-phase depletion. The surface tension equation is here extrapolated outside the range of compositions constrained by the data of Kristensen et al. (2014) and Lin et al. (2020) and the validity of the explicit salt term and accompanying fit parameter values is not confirmed for these solution states. This constraint on model parameters for droplet states predicted with consideration of bulk/surface partitioning is a remaining challenge for all droplet partitioning frameworks, regardless of whether bulk or surface composition based thermodynamic relations are used. Model (B) is less sensitive to the ternary fit equation, as droplets are more dilute, but notably have compositions much better constrained by the data underlying the fits. Using the explicit

salt terms lead to slightly higher predicted critical supersaturations, but notably far from able to reconcile the severe underestimations of  $SS_c$  generally observed with (B).

## S6.5 Small amounts of impurities in NAFA

Small amounts of soluble impurities can significantly enhance organic aerosol CCN activity, from increased hygroscopic properties of the overall particle (Bilde and Svenningsson, 2004). The sensitivity of models (P), (S), (B) and (K) was tested to the assumption of 3 and 5% by mass of NaCl impurity present in the NAFA sample. Results are shown in Fig. S8 against the corresponding calculations assuming 100% NAFA (base case) and experimental values from Kristensen et al. (2014) for pure NAFA particles. Indeed, a relatively small amount of only 3% of NAFA comprised by NaCl essentially reconcile both the partitioning model (P) and the simple partitioning model (S) with experimental values. For mixed NAFA–NaCl particles, change of composition from the nominal value could arise not only from an actual contamination or deterioration of the NAFA sample during experiments, but also from bias in the fractionation of solute composition introduced in the nebulizer during particle production, which could change the resulting dried particle composition from that of the solute in the stock solution from which particles were generated. More details on the experimental methods are provided by Kristensen et al. (2014). Such a phenomenon has been observed by Brooks et al. (2004) for organic–inorganic mixtures.

It can be seen from Fig. S8 that the size dependency of the Köhler model calculations in this work has a slightly different slope than the experimental data of Kristensen et al. (2014), and assuming a 3% NaCl impurity leads to slight underestimations of critical supersaturations for the smallest particles and conversely to slight overestimations in the high particle size end. A composition fractionation as reported by Brooks et al. (2004) could very well vary in degree with the size of the particles produced, with smaller particles less depleted or even enriched in the surface active component, since these particles are also created from smaller nebulized droplets. This mechanism would explain the observed relative trends.

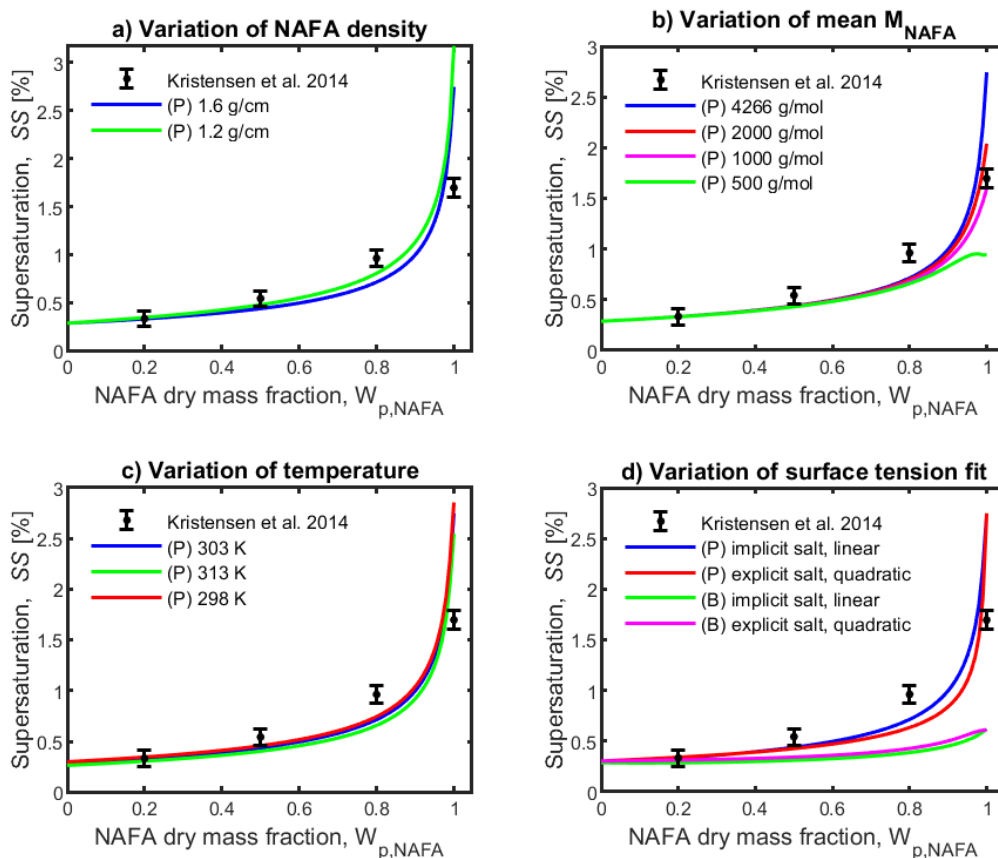


Figure S7: Sensitivity of the Köhler model calculations described in Sections 2.1–2.4 to various input parameters: Sensitivity of the full mass-based partitioning framework described in Sections 2.1–2.3 to (a) assumed mass density of NAFA, (b) estimated average value of NAFA molar mass, and (c) temperature variations estimated inside the CCNC instrument during measurements of droplet activation. (d) Sensitivity of models (P) and (B) to fitting equations for ternary surface tension, including implicit and explicit binary salt term, and linear and quadratic equations for the Szyszkowski surface tension parameters. Experimental critical supersaturations reported by Kristensen et al. (2014) are shown in each panel for reference. Details of the parameter variations and model sensitivities are given in Section S6.

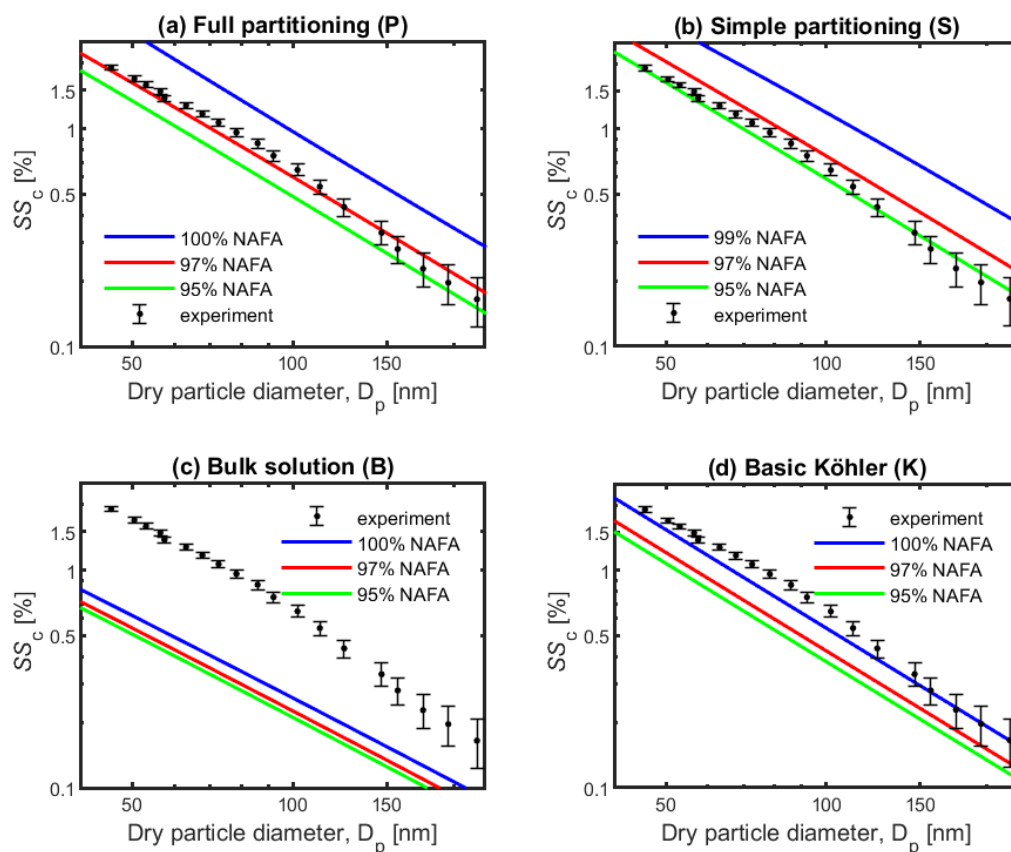


Figure S8: Sensitivity of the Köhler model calculations described in Sections 2.1–2.4 to small amounts of impurities in the NAFA sample, exemplified by 3% and 5% by mass of NaCl in nominally pure NAFA particles: (a) the comprehensive partitioning model (P), (b) the simple partitioning model (S), (c) the bulk solutions model (B) and (d) the basic Köhler model (K). For model (S), calculations with 99% NAFA are shown instead of pure NAFA particles, because the model cannot be applied in the limit  $W_{p,NAFA} \rightarrow 0$ .

## References

- Alvarez, N. J., Walker, L. M., and Anna, S. L.: A Microtensiometer To Probe the Effect of Radius of Curvature on Surfactant Transport to a Spherical Interface, *Langmuir*, 26, 13 310–13 319, <https://doi.org/10.1021/la101870m>, URL <https://doi.org/10.1021/la101870m>, PMID: 20695573, 2010.
- Alvarez, N. J., Walker, L. M., and Anna, S. L.: A criterion to assess the impact of confined volumes on surfactant transport to liquid–fluid interfaces, *Soft Matter*, 8, 8917–8925, <https://doi.org/10.1039/C2SM25447F>, URL <http://dx.doi.org/10.1039/C2SM25447F>, 2012.
- Aumann, E., Hildemann, L., and Tabazadeh, A.: Measuring and modeling the composition and temperature-dependence of surface tension for organic solutions, *Atmospheric Environment*, 44, 329–337, 1967.
- Bilde, M. and Svenningsson, B.: CCN Activation of Slightly Soluble Organics: The Importance of Small Amounts of Inorganic Salt and Particle Phase, *Tellus*, 56B, 128–134, 2004.
- Brooks, S. D., DeMott, P. J., and Kreidenweis, S. M.: Water uptake by particles containing humic materials and mixtures of humic materials with ammonium sulfate, *Atmospheric Environment*, 38, 1859–1868, 2004.
- Coltharp, K. A. and Franses, E. I.: Equilibrium and dynamic surface tension behavior of aqueous soaps: sodium octanoate and sodium dodecanoate (sodium laurate), *Colloids and Surfaces A: Physicochemical and Engineering Aspects*, 108, 225–242, 1996.
- Davies, J. F., Zuend, A., and Wilson, K. R.: Technical note: The role of evolving surface tension in the formation of cloud droplets, *Atmospheric Chemistry and Physics*, 19, 2933–2946, 2019.
- Dillmann, A. and Meier, G. E. A.: A refined droplet approach to the problem of homogeneous nucleation from the vapor phase, *The Journal of Chemical Physics*, 94, 3872–3884, <https://doi.org/10.1063/1.460663>, URL <https://doi.org/10.1063/1.460663>, 1991.
- Dinar, E., Mentel, T. F., and Rudich, Y.: The density of humic acids and humic like substances (HULIS) from fresh and aged wood burning and pollution aerosol particles, *Atmospheric Chemistry and Physics*, 6, 5213–5224, 2006.

- Fainerman, V. B., Miller, R., and Möhwald, H.: General Relationships of the Adsorption Behavior of Surfactants at the Water/Air Interface, *J. Phys. Chem. B*, 106, 809–819, 2002.
- Kiss, G., Tombacz, E., Varga, B., Alsberg, T., and Persson, L.: Estimation of the average molecular weight of humic-like substances isolated from fine atmospheric aerosol, *Atmospheric Environment*, 37, 3783–3794, 2003.
- Kiss, G., Tombacz, E., and Hansson, H.-C.: Surface Tension Effects of Humic-Like Substances in the Aqueous Extract of Tropospheric Fine Aerosol, *Journal of Atmospheric Chemistry*, 50, 279–294, 2005.
- Kristensen, T. B., Prisle, N. L., and Bilde, M.: Cloud droplet activation of mixed model HULIS and NaCl particles: Experimental results and  $\kappa$ -Köhler theory, *Atmospheric Research*, 137, 167–175, 2014.
- Lin, J. J., Kristensen, T. B., Calderón, S. M., Malila, J., and Prisle, N. L.: Effects of surface tension time-evolution for CCN activation of a complex organic surfactant, *Environmental Science: Processes & Impacts*, 22, 271–284, 2020.
- Low, R.: A Theoretical Study of Nineteen Condensation Nuclei, *Journal de Recherches Atmospheriques*, pp. 65–78, 1969.
- Mäkelä, J. and Manninen, P.: Molecular size distribution and structure investigations of humic substances in groundwater, working report 2008-36, Posiva Oy, Posiva Oy, Olkiluoto, FI-27160 Eurajoki, Finland, 2008.
- Noziere, B., Baduel, C., and Jaffrezo, J.-L.: The dynamic surface tension of atmospheric aerosol surfactants reveals new aspects of cloud activation, *Nature Communications*, 5, 1–7, 2014.
- Prisle, N. L., Raatikainen, T., Sorjamaa, R., Svenningsson, B., Laaksonen, A., and Bilde, M.: Surfactant partitioning in cloud droplet activation: a study of C8, C10, C12 and C14 normal fatty acid sodium salts, *Tellus*, 60B, 416–431, <https://doi.org/10.1111/j.1600-0889.2008.00352.x>, 2008.
- Prisle, N. L., Raatikainen, T., Laaksonen, A., and Bilde, M.: Surfactants in cloud droplet activation: mixed organic-inorganic particles, *Atmos. Chem. Phys.*, 10, 5663–5683, <https://doi.org/10.5194/acp-10-5663-2010>, 2010.
- Ruehl, C. R., Davies, J. F., and Wilson, K. R.: An interfacial mechanism for cloud droplet formation on organic aerosols, *Science*, 351, 1447–1450, <https://doi.org/10.1126/science.aad4889>, URL <http://science.sciencemag.org/content/351/6280/1447>, 2016.

- Szyskowski, B. V.: Experimentelle studien über kapillare eigenschaften der wässerigen lösungen von fettsauren, *Zeitschrift für Physikalische Chemie*, 64, 385–414, 1908.
- Tuckermann, R.: Surface tension of aqueous solutions of water-soluble organic and inorganic compounds, *Atmospheric Environment*, 41, 6265–6275, 2007.
- Van den Bogaert, R. and Joos, P.: Dynamic surface tensions of sodium myristate solutions, *The Journal of Physical Chemistry*, 83, 2244–2248, 1979.
- Van den Bogaert, R. and Joos, P.: Diffusion-controlled adsorption kinetics for a mixture of surface active agents at the solution-air interface, *The Journal of Physical Chemistry*, 84, 190–194, 1980.
- Vanhanen, J., Hyvärinen, A.-P., Anttila, T., Raatikainen, T., Viisanen, Y., and Lihavainen, H.: Ternary solution of sodium chloride, succinic acid and water; surface tension and its influence on cloud droplet activation, *Atmospheric Chemistry and Physics*, 8, 4595–4604, 2008.
- Wen, X. Y., McGinnis, K. C., and Franses, E. I.: Unusually low dynamic surface tensions of aqueous solutions of sodium myristate, *Colloids and Surfaces A: Physicochemical and Engineering Aspects*, 143, 371–380, 1998.